

# Improvements to Siemens Eclipse PET Cyclotron Penning Ion Source

D. Potkins<sup>1, a)</sup>, M. Dehnel<sup>1</sup>, S. Melanson<sup>1</sup>, T. Stewart<sup>1</sup>,  
J. Hinderer<sup>2</sup>, N. Jones<sup>2</sup>, L. Williams<sup>2</sup>

<sup>1</sup>*D-Pace Inc., Suite 305, 625 Front St., Nelson, BC, V1L 4B6, Canada*

<sup>2</sup>*Siemens Molecular Imaging, 810 Innovation Drive, Knoxville, TN, 37932, USA*

*<sup>a)</sup>Corresponding author: dave@d-pace.com*

**Abstract.** The Siemens Eclipse (RDS111) cyclotron utilizes an internal Penning Ion Gauge (PIG) ion source to provide the negative hydrogen ions for this 11 MeV PET cyclotron. Siemens worked with D-Pace Inc. to optimize the ion source current and transmission through the cyclotron to the radioisotope targets. The goal was to increase the target current from 120  $\mu\text{A}$  (dual 60 $\mu\text{A}$ ) to 150 $\mu\text{A}$  (dual 75 $\mu\text{A}$ ) and to increase the time between ion source rebuilds from 120 hours to 300 hours. Over 80 experiments were conducted including tests on ion sources with modified cathode, anode, and puller lens geometries and materials, hydrogen gas flow configurations, and a biased plasma lens design. Cesium was introduced to the ion source which alone increased the beam current on target by over 20%. These short-term tests are being followed up with longer duration field testing.

## INTRODUCTION

The Siemens Eclipse (RDS111) cyclotron utilizes an internal Penning Ion Gauge (PIG) ion source to provide the negative hydrogen ions for this 11 MeV PET cyclotron. This ion source was developed three decades ago for the production of PET radioisotopes, and since then, the design has remained largely unchanged. The goal of this project was to increase the total target current from 120  $\mu\text{A}$  (dual 60  $\mu\text{A}$ ) to 150  $\mu\text{A}$  (dual 75  $\mu\text{A}$ ) and to increase the time between ion source rebuilds from 120 hours to more than 300 hours.

The project presented a rare opportunity of near-exclusive access to this industrial cyclotron to conduct a large number of experiments to test different configurations of the ion source. Siemens part suppliers were able to quickly manufacture variants of key components of the ion source, and over 80 tests were conducted.

## SIEMENS RDS111 PENNING ION SOURCE

The RDS111 Penning ion source is a ‘cold’ cathode design. Two opposing cathodes are biased at a negative potential (-0.5 to -3 kV) relative to the anode. The anode is made up of three parts: the hourglass-shaped anode body and two identical collimators at each end (Fig. 1). The anode body and collimators are at the ion source bias potential of -17 kV relative to ground. Electrons emitted by the self-heated cathodes oscillate between the two cathodes. The four-sector cyclotron magnet has a ~0.7 Tesla field in center of the cyclotron where the Penning ion source is located, and this field largely traps the electrons emitted from the cathodes in a tight column of approximately the same diameter ( $\varnothing$ 4 mm) as the collimator apertures (Fig. 1).

The arc power supply provides the necessary arc current to maintain the plasma within the anode. To initiate the arc, a high voltage (up to -3 kV) is applied to the cathodes. Primary electrons are emitted from the cathodes, which ionize the gas, forming positive ions ( $H^+$  and  $H^{2+}$ ). The positive ions accelerate back to the cathodes, causing the cathodes to heat until the cathodes reach a temperature at which they are said to have become ‘thermionic’. Once thermionic, the electron emission from the cathodes is sufficient to maintain the hot plasma within the anode.  $H^-$  ions are extracted through the slit in the anode by the puller lens, which is held at ground potential. When the cyclotron RF is off, the DC beam strikes an electrically isolated graphite post (Fig. 2) where the ion source extracted beam current can be measured. This current is referred to as beam-on-post (BoP). When the cyclotron RF is on, only the beam near the peak of the RF waveform is accelerated through 78 cyclotron turns to the stripper foils, then through the collimators to the targets. This current is referred to as the target current. The ratio of stripper-foil current divided by beam-on-post current provides an indication of transmission efficiency between the ion source, through the cyclotron, to the foil. A typical post-to-foil transmission for the cyclotron is 18% to 20%. The beam lost on the collimators between the stripper foil and the target results in a typical foil-to-target transmission of 80%.

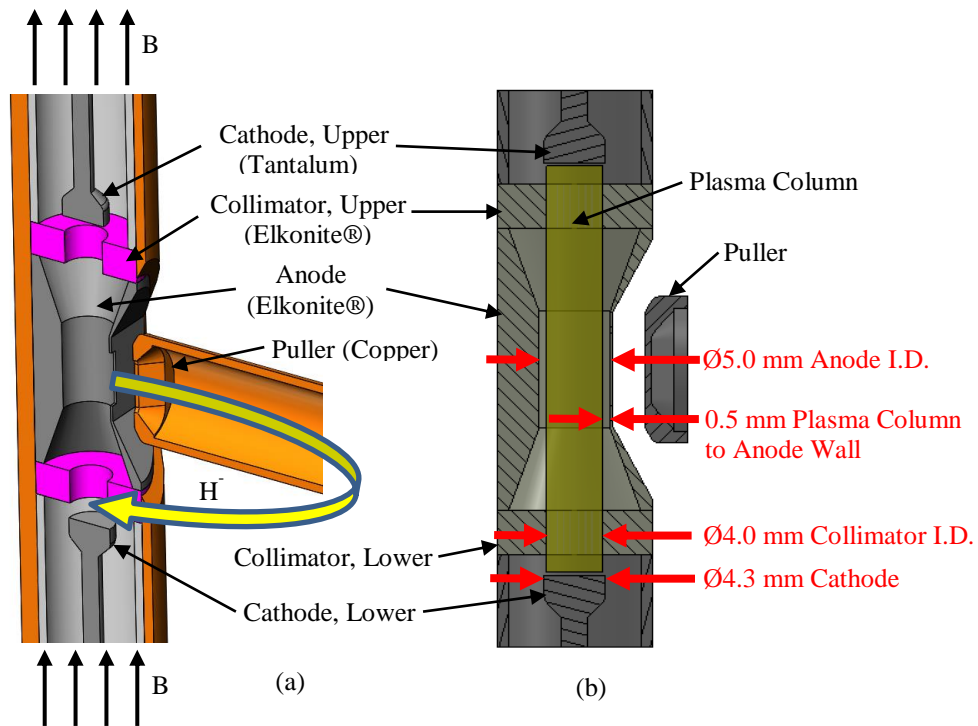


**FIGURE 1.** Isometric (a) and section (b) views of the RDS111 Penning ion source. Plasma column diameter is defined by the collimators, which have inside diameter of 4.0 mm.

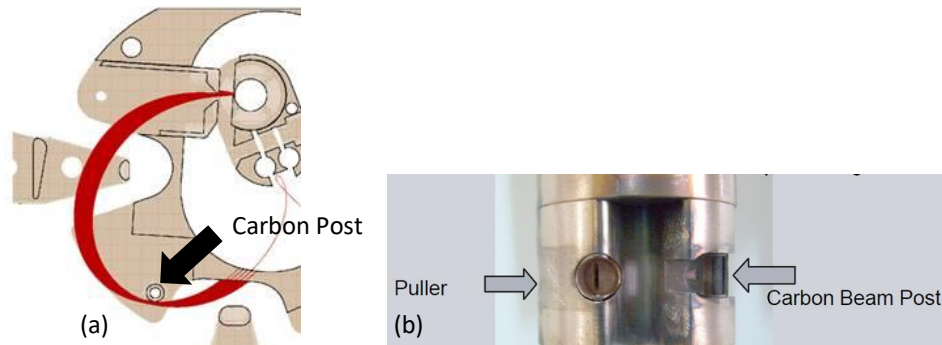


**FIGURE 2.** (a) Simion™ simulation of beam on post, with extraction voltage = 15 kV (showing the beam just missing the post for this anode-puller position configuration), (b) carbon post

## EXPERIMENTS

A series of experiments were conducted using three different ion sources. The most significant challenge of the project was the variability introduced by rebuilding and installation of the ion sources between experiments, and the gradual reduction of beam current as the collimators and anode are eroded as the ion source ages following an ion source rebuild. Baseline experiments of the standard configuration of the ion source were interleaved between ion source variant experiments, but experiment-to-experiment variability was 5% for the same ion source configuration and 10% or more between rebuilds.

Most experiments were conducted with a constant arc current of 0.27 Amps, which is the typical arc current required to produce 120  $\mu\text{A}$  total target current on two targets. For each experiment, gas flow, bias voltage, and RF voltage were tuned to maximize target current. Parameter sweeps were also conducted, with bias voltage swept from -15.4 kV to -17.4 kV,  $\text{H}_2$  gas from 3.5 sccm to 7.5 sccm, and RF voltage from 36.2 kV to 38.2 kV. Ion source position relative to the puller lens was also optimized. Beam-on-post was measured with the RF power off, bias voltage at -15 kV, and the gas flow rate set to the same flow rate used to optimize for the maximum target current.

**TABLE 1.** Typical operating parameters of ion source and cyclotron for 120  $\mu\text{A}$  beam current on target

Parameter	
Bias Voltage	17 kV
Bias Current	7.6 mA
$\text{H}_2$ Gas Flow	5.5 sccm
RF Frequency	72.5 MHz
RF Amplitude	36.8 kV
RF Power	8.8 kW
Dipole Magnet Current	224.6 A
Arc Current	0.27 A
Arc Voltage	550 V
Arc Power	150 W
Beam-on-Post (Extraction Current)	800 $\mu\text{A}$
Post-to-Stripper-Foil Transmission	18-20%
Stripper-Foil-to-Target Transmission	75-85%
Main Tank Vacuum	4e-6 Torr

### Plasma Column Geometry Modifications

The  $\text{H}^-$  ions are thought to be produced through dissociative electron attachment in the plasma volume. This requires an electron temperature of 0.7 eV, matching the binding energy of the second electron which forms  $\text{H}^-$  [1]. The space between the inner wall of the anode and the plasma column creates this ‘cool’ plasma region required for  $\text{H}^-$  volume formation. This distance was optimized by the original designers of the ion source to be 0.7 mm [1], though for the nominal Siemens design this space was only 0.5 mm (Fig. 1b). Experiments were conducted to measure the effects of changing the plasma-column-to-anode-wall distance by altering the inner diameters of the collimators or anode.

An increase of target current (+6%) was observed with a reduction of the collimator aperture diameter from 4.0 mm to 3.8 mm (increased ‘cool’ region from 0.5 mm to 0.7 mm). There was negligible change in target current with an increase in collimator diameter from 4.0 mm to 4.2 mm (decreased ‘cool’ region from 0.5 mm to 0.3 mm). Interestingly, increasing the anode diameter from 4.0 mm to 4.2 mm (also increases ‘cool’ region from 0.5 mm to 0.7 mm) yielded negligible improvements. Further experiments using larger aperture increments were recommended.

## Anode & Puller Slit Area Variations

Experiments were performed with the same extraction aperture length-to-width aspect ratio, but with varied slit-aperture areas. There was ‘anecdotal’ evidence that -10% anode and puller slit area reductions resulted in increased (+5%) target beam current and +10% slit area increases reduced (-5%) target beam current, but the large degree of variability between repeated experiments made this testing inconclusive. The nominal anode slit is rectangular, 0.7 mm x 5.2 mm. The nominal puller slit is a full-radii slot 1.1 mm x 5.3 mm. The anode-to-puller distance is nominally 2.3 mm, though this is optimized during tuning.

An experiment was conducted with round apertures ( $\text{Ø}2.1$  mm anode and  $\text{Ø}2.7$  mm puller) with the same cross section areas as their rectangular-baseline counterparts. Post-to-foil transmission increased dramatically (from 19% to 30%) but the total target current decreased from 120  $\mu\text{A}$  to 40  $\mu\text{A}$ . The optimized position of the anode-puller following maximization of beam current is shown in Fig. 3. The offset between the anode and puller apertures is likely a result of the optimized relative positions restricting the gas flow from the ion source into the central region of the cyclotron, where  $\text{H}^-$  stripping occurs. The likely reason for the 57% post-to-foil transmission increase was the improved acceptance of the vertically-shortened ion beam through the cyclotron.

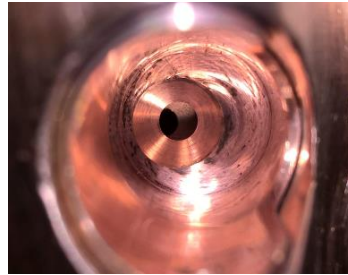


**FIGURE 3.** Round aperture puller (foreground) and anode (background) following beam current optimization

## Increasing Surface Area Near Anode Slit

It was hypothesized that an increase in the surface area of the anode near the anode-exit slit would improve  $\text{H}^-$  surface production. Several methods of increasing the surface area were tested (Figure 4) including texturing the interior of the anode by ‘media blasting’, and by adding machined features near the anode slit. The machined features added approximately 15% surface area in the slit region. Texturing did not affect the ion source performance. Surface area increases in the Elkonite® anode also resulted in negligible beam current increases. However, anodes made from molybdenum with circumferential groove features lowered the arc power by 7% and increased the target beam current by 20%. An anode made from molybdenum without the groove features resulted in a beam current increase of only 6%, and this increase is relative to a baseline measurement made a month prior and should be repeated. Further testing with grooved molybdenum anodes was recommended.

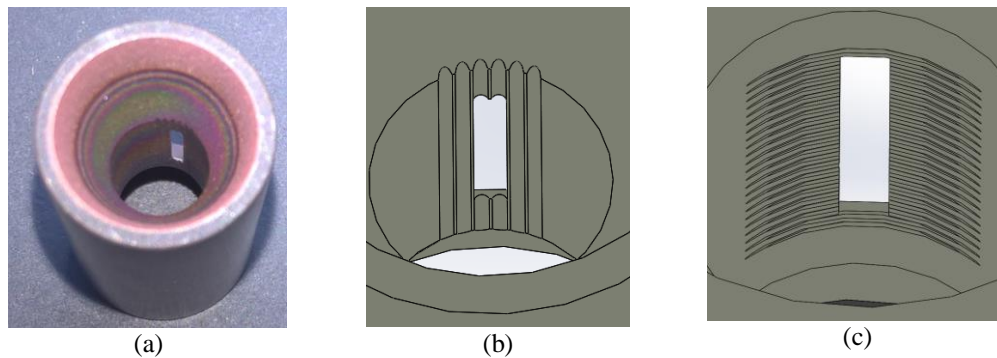


**FIGURE 4.** Surface modification to anode slit area. (a) Anode interior textured with ‘media’ blasting (b) 6 vertical grooves, 0.13 mm deep, (c) 22 circumference grooves, 0.08 mm deep, pitch 0.254 mm

**TABLE 1.** Results of testing anodes with modified inner surfaces and materials

Test Description	Test Number	Bias Current (mA)	Arc Power (W)	BoP (mA)	Transmission Post-to-Foil %	Beam Current on Target ( $\mu$ A)
Baseline, 07/17/2017	50	7.0	146	925	17.3	125
Baseline, 8/10/2017	64	7.6	151	806	19.9	128
Threaded Anode, Elkonite®, 07/11/2017	46	5.5	149	822	19.8	133
Threaded Anode, Elkonite®, 08/23/2017	71	6.6	144	772	19.7	121
Slotted Anode, Ta, 06/30/2017	42	6.5	153	877	18.2	124
Threaded Anode, Moly, 08/16/2017	67	5.9	139	1050	18.8	154
Threaded Anode, Moly, 08/17/2017	68	6.4	137	1026	18.7	150
Standard Anode, Moly, 09/29/2017	83	6.1	165	794	21.3	136

### Thoriated Tungsten Cathodes

Thoriated tungsten cathodes were fabricated to increase the emitted electron density by lowering the work function of the cathode material. Thoriated tungsten has a work function of 2.63 eV compared to 4.12 eV for tantalum [2]. However, tungsten has a higher thermal conductivity (170 W/mK) than tantalum (60 W/mK), so it was necessary to reduce the conducted heat lost from the tungsten cathode head to the cathode body. Two approaches were used. The first was to construct a composite cathode consisting of a tantalum base, a low-thermal-conductivity graphite (EK40, SGL Carbon Group) neck ( $\text{\O}2.5$  mm), and a thoriated-tungsten head (Fig. 5a). A second approach was to reduce conductive heat loss by decreasing the cathode neck from  $\text{\O}1.6$  mm to  $\text{\O}1.1$  mm (Fig. 5b). The graphite-necked-tungsten cathode resulted in -17% target current and +20% arc power. The  $\text{\O}1.1$  neck thoriated-tungsten-head cathode resulted in no changes in target current but required +28% more arc power.

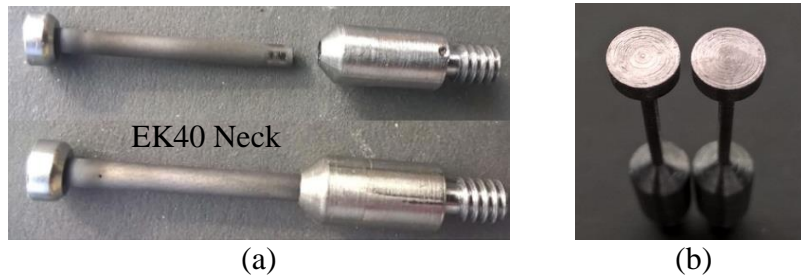


**FIGURE 5.** (a) Composite cathode tantalum base, EK40 graphite neck and thoriated tungsten head, (b) Cathode neck reduced from 1.6mm to 1.1mm

### Cesium

Cesium is commonly used in ion sources to enhance the  $\text{H}^-$  surface production in ion sources [3]. The work function of bulk cesium is 2.1 eV. If a molybdenum surface is partially coated with cesium, the work function of a molybdenum surface decreases from 4.6 eV to 1.5 eV [4]. Cesium getters from SAES Group were used instead of elemental cesium for practical and safety reasons. Each of the 2.7 mg,  $\text{\O}1$  mm x 0.8 mm thick pills contained 0.6 mg of cesium. The cesium is released from the Cs-Al-Zr salt at temperatures exceeding 550°C. Since the ion source was too small to implement electrically-powered getter heaters, the pill needed to be placed in a location which exceeded 550°C. The Cs pill (Fig. 6a) was tested installed in the collimator (Fig. 6b), and installed in the cathode (Fig. 6c).

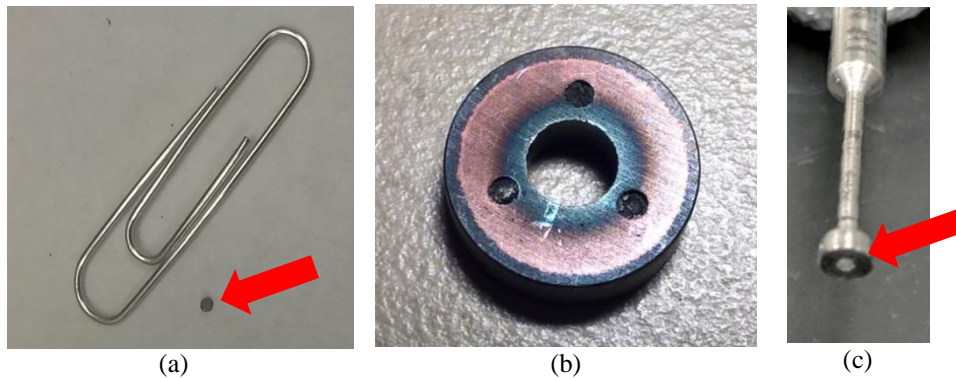


**FIGURE 6.** (a) Cesium getter pill, (b) Cesium getters installed in collimator, (c) Cesium getter installed in cathode

The ion source was cesiated by setting the arc current to 0.1 A and operating the ion source to heat the cathode and cesium getter for 10 minutes with no bias voltage or RF power. The arc was then extinguished, and the ion source was cooled for 20 minutes to allow the cesium to condense within the ion source. The ion source was then restarted normally. This cesiation process was not optimized. A standard Elkonite® anode was used.

With one Cs pill installed in the tantalum lower cathode, the beam current on target increased from 123  $\mu\text{A}$  to 155  $\mu\text{A}$ . The arc power decreased from typical values in the range of 145 to 170 W, to 116 W. The ion source was then run for two hours while controlling the target beam current setpoint to 150  $\mu\text{A}$ . Over this period, the arc power increased from 106 W to 112 W, the bias current increased from 8.8 mA to 9.5 mA, and the arc current increased from 0.25 A to 0.26 A (Fig. 7). Siemens has initiated field studies utilizing cesium getters based on these promising results. Testing the ion source with cesium and a molybdenum anode with circumferential-groove features near the exit slit is pending.

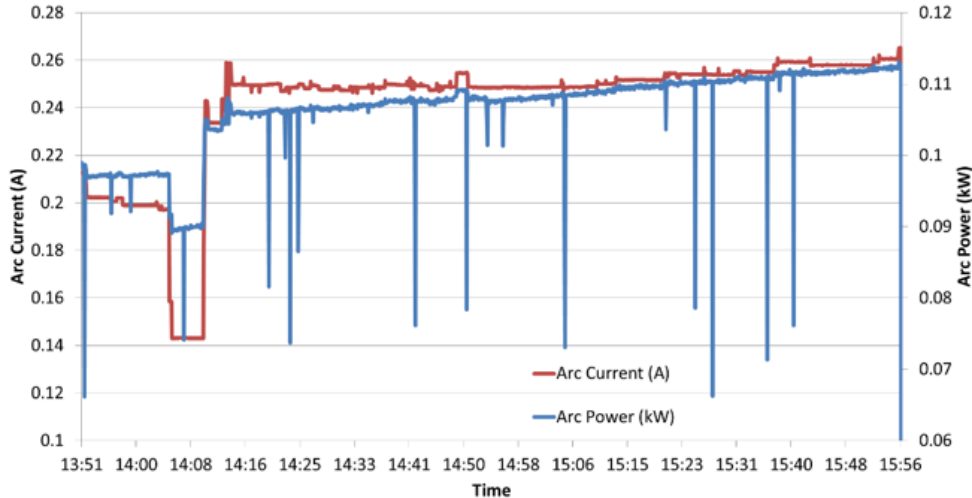


**FIGURE 7.** Following an initial reduction of arc power (-25%) and an increase in beam current (+26%) after cesiation, the arc current and power gradually increased over a two-hour ion source operation (for target beam current controlled to a set point of 150  $\mu\text{A}$  by varying arc current).

**TABLE 1.** Beam current and arc power improvements with the addition of cesium getters, using tantalum cathodes, and arc current of 0.27 A

Test Description	Test Number	Bias Current (mA)	Arc Power (W)	BoP (mA)	Transmission Post-to-Foil %	Beam Current on Target ( $\mu\text{A}$ )
Baseline, 7/18/2017	51	7.5	182	832	18.6	124
1 Cs pill, lower collimator, 07/27/2017	58	6.7	162	836	20.4	127
3 Cs pills, lower collimator, 09/08/2017	75	8.2	167	823	21.2	140
1 Cs pill, lower cathode, 09/07/2017	74	9.9	116	925	20.3	155

### Biased Anode (Plasma Electrode)

Jimbo et al. [5] found that the extracted-negative-ion current increased with decreasing bias voltage on the anode-exit slit, with a maximum beam current at an anode bias voltage of -6 V for their ion source configuration. This was a doubling of their  $\text{H}^-$  current, but also resulted in increased co-extracted electron current. To test this concept with the Siemens Penning ion source, an ion source was modified so the anode slit could be biased between +10 V and -10 V by shortening the anode and adding ceramic insulators between the collimator and the anode body (Fig. 8). We referred to this configuration as the plasma-electrode configuration.

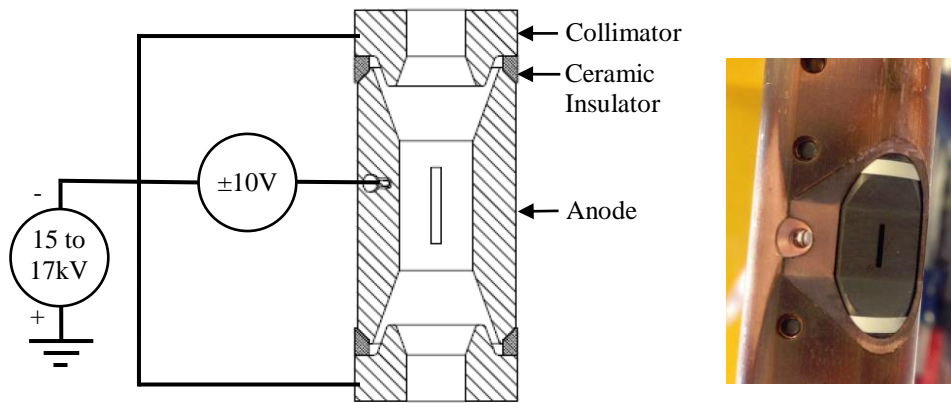


**FIGURE 8.** Plasma electrode – biased anode slit

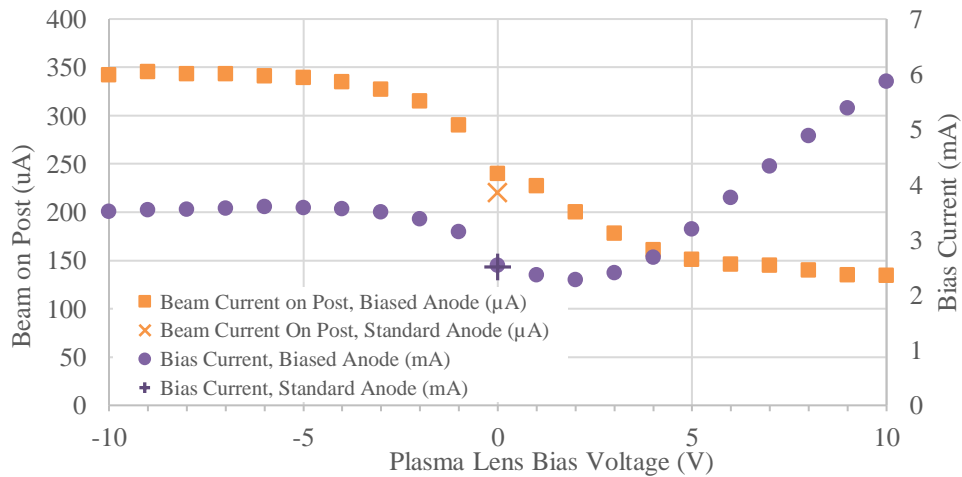


**FIGURE 9.** Increase of 30% beam-on-post with anode negative biased relative to collimators. Arc current = 0.11 Amps, ion source bias = 15.3 kV,  $\text{H}_2$  gas = 5.5 sccm

As with the baseline design, both the collimators and anodes were made from Elkonite®. For the first test, the ion source was operated at 0.11 A arc current (instead of 0.27 A) to ensure the anode and connecting wire were not thermally damaged, because the biased anode did not contact the water-cooled ion source tube as it does in its standard configuration. Figure 9 shows an increase of 30% in beam on post when the plasma-electrode bias voltage was changed from 0 V to -9 V relative to the collimators, while the ion source bias current increased from 2.4 mA to 3.5 mA over this same voltage range.

However, when the ion source was operated with 0.27 A arc current, the beam on target was only 67  $\mu\text{A}$  with no plasma-electrode bias voltage and increased to 74  $\mu\text{A}$  with plasma-lens bias of -10 V and a post-to-foil transmission of 11%. The target current and post-to-foil transmission for this arc current of 0.27 A for the standard ion source configuration are 120  $\mu\text{A}$  and 20% respectively. The increase in co-extracted electrons from the biased anode slit likely increases space charge and resulted in poor transmission through the cyclotron. Also, since the modified anode was thermally isolated from the cooled housing, the anode was likely very hot, and high temperatures of the anode may have impacted  $\text{H}^-$  surface production. A means of cooling the electrically-isolated anode would be required. The plasma lens concept was not pursued further due to the significant engineering and retrofitting challenges involved with implementing this change.

## CONCLUSIONS

D-Pace recommended that Siemens conduct addition testing to determine the effects of combining configuration changes which yielded improvements in the current study, when combined in a single ion source. D-Pace also recommended conducting long-term testing to determine the effects of these changes on ion source life time. These configurations include:

1. Collimators with inside diameter reduced by -10% area to achieve 0.7 mm ‘cool’ region
2. Re-test anode & puller slits with -10% area, including experiments with changes to slit aspect ratio
3. Conduct further tests with molybdenum anodes with circumference groove features near the exit slit
4. Retest the ion source with molybdenum cathodes and cesium getters
5. Conduct field test on customer cyclotrons to verify improvements on other cyclotrons

## ACKNOWLEDGMENTS

D-Pace thanks Siemens Molecular Imaging co-authors James Hinderer for the opportunity to work with Siemens on this project and for his enthusiasm to pursue the wide range recommended tests, Nathan Jones for his ion source tuning experience, and Logan Williams for his meticulous design and coordination skills.

## REFERENCES

1. L. Carroll and F. Ramsey, “RDS111 Ion source system – theory of operation”, Siemens internal document, (1994) (unpublished).
2. R. Scrivens, “Electron and ion sources for particle accelerators,” CAS CERN-2006-002, pp. 495-504 (2006), available at <https://cds.cern.ch/record/941321>.
3. Y. Belchenko, G. Dimov, V. Dudnikov, Nuclear Fusion vol. 14, no. 1, pp. 113-114 (1974).
4. D. Faircloth, “Negative Ion Sources: Magnetron and Penning,” CERN Yellow Report CERN-2013-007, pp. 285-310 (2013), available at <http://cds.cern.ch/record/1693328>.
5. K. Jimbo, K. W. Ehlers, K. N. Leung, and R. V. Pyle, Nuclear Instruments and Methods in Physics Research A vol. 248, pp. 282-286 (1986).